



Vegetation changes and formation of small-scale urban heat islands in three populated districts of Kerala State, India

Bijeesh Kozhikkodan Veettil^{1,2} · Atilio Efrain Bica Grondona³

Received: 21 March 2018 / Accepted: 2 August 2018 / Published online: 10 August 2018
© Institute of Geophysics, Polish Academy of Sciences & Polish Academy of Sciences 2018

Abstract

Currently, more than half of the world's population is living in cities. Rapid and unplanned urbanization became a common scenario in rapidly developing countries such as those in Asia. Decline in vegetation coverage and increase in local air and land surface temperatures are among the adverse effects of unplanned urban growth. We used Landsat data for the period 1991–2017 to estimate the expansion of urban areas in terms of vegetation loss and the development of small-scale urban heat islands in developing cities in Kerala state of India. For the last 27 years, unplanned urbanization in Kerala state has increased and this resulted in the enhanced loss of vegetation and, possibly, resulted in the increase in land surface temperature (LST). Our results indicate that vegetation coverage, particularly near the urban areas, has been decreased by 5.8%, 10.4%, and 9.6% in Ernakulam, Trichur, and Kozhikode districts, respectively. The land surface temperatures also have been increased during the study period. It is interesting to note that higher increase in LST and higher reduction in vegetation coverage were observed in Trichur and Kozhikode districts compared with highly populated and urbanized Ernakulam district.

Keywords Land surface temperature · Landsat · Urban sprawl · Urban heat island · Vegetation cover

Introduction

Since the nineteenth century, global mean temperature has increased and major cities have been emerged as a consequence of industrialization and rapid urbanization (Grondona et al. 2013). Currently, more than half of the world's population is living in cities (Cohen 2003). Compared to the developed countries in North America and Europe, population living in urban settlements is smaller in Asia (UN 2014, 2016). However, rapid urbanization is currently undergoing in Asian region and the population in urban

areas in Asia is supposed to increase 64% by 2025 (UN 2014). Urbanization improves the quality of life and economic growth in fast developing countries. On the other hand, urban growth without proper planning has profound impact on the environment (Ranagalage et al. 2014). Urban sprawl in the suburban areas also possesses the same adverse effects as urban growth on the environment. The adverse effects of urbanization and urban sprawl on the environment include loss of vegetation, microorganisms, habitat and water bodies, pollution and greenhouse emission, formation of urban heat islands (UHI), biodiversity degradation, influence on ecological and biogeochemical cycles and spread of diseases (Estoque and Murayama 2014; Son and Thanh 2018).

The most visible effects of rapid urbanization are the loss of vegetation cover and increase in concrete infrastructures (Carlson and Arthur 2000; Du et al. 2010). In other words, changes in land cover and vegetation can be used to monitor the growth of urban settlements.

Urban heat island can be defined as the appearance of a higher atmospheric and land surface temperatures in urban areas compared to the surrounding rural areas (Voogt and

✉ Bijeesh Kozhikkodan Veettil
bijeesh.veettil@tdt.edu.vn

¹ Department for Management of Science and Technology Development, Ton Duc Thang University, Ho Chi Minh City, Vietnam

² Faculty of Environment and Labour Safety, Ton Duc Thang University, Ho Chi Minh City, Vietnam

³ Centro Estadual de Pesquisas em Sensoriamento Remoto e Meteorologia, Universidade Federal do Rio Grande do Sul (UFRGS), Porto Alegre, Brazil

Oke 2003). Two types of UHIs observed are: surface urban heat island (SUHI), which is observed based on LST and atmospheric urban heat island (AUHI), which is normally measured based on the air temperature (Ranagalage et al. 2014). It is observed by some researchers (e.g., Chen et al. 2006) that UHI is stronger in the autumn and winter than the summer months.

The two major adverse effects of rapid urban growth described above—vegetation loss (or formation of new settlements) and SUHI formation—can be estimated effectively using remote sensing data (Veettil 2012; Grondona et al. 2013). In this study, we estimated the expansion of urban areas by means of vegetation loss in three populated districts in India and SUHI using multi-spectral satellite imagery in the same area. Despite the limitations due to spatial resolution of the data used, remote sensing methods are still efficient by eliminating the problems associated with multiple user data interpretation and is faster compared to other traditional methods for estimating LST (Grondona et al. 2013).

Study site

In this study, the growth of urban areas by means of vegetation cover changes in three highly populated districts in Kerala state of India (Trivandrum, Ernakulam, and Kozhikode) for the period 1991–2017 was estimated using Landsat image series. The Indian state of Kerala is considered as the fourth most urbanized state in India for the period 2001–2011 (Sudhira and Gururaja 2012). Development of small-scale UHIs associated with urban sprawl during the same period was also analyzed using the same satellite data (Fig. 1).

It has been reported that Kozhikode and Ernakulam were ranked among the 20 most populated cities in India in 2011 (based on census 2011 data) and these two showed a significant population rise rate during 2001–2011 (Sudhira and Gururaja 2012). At the same time, overall population rise in Kerala was very small (5%) compared with the urban population growth (48%), and there was a significant decline in rural population (25%) (Sudhira and Gururaja 2012).

Data and methods

Landsat image series (Thematic Mapper—TM, Enhanced Thematic Mapper Plus—ETM+, and Operational Land Imager—OLI) acquired between 1991 and 2017, having a spatial resolution of 30 m in multispectral channels except thermal wavelengths, were used for this research. Spatial resolution of thermal bands in TM, ETM+ and OLI are

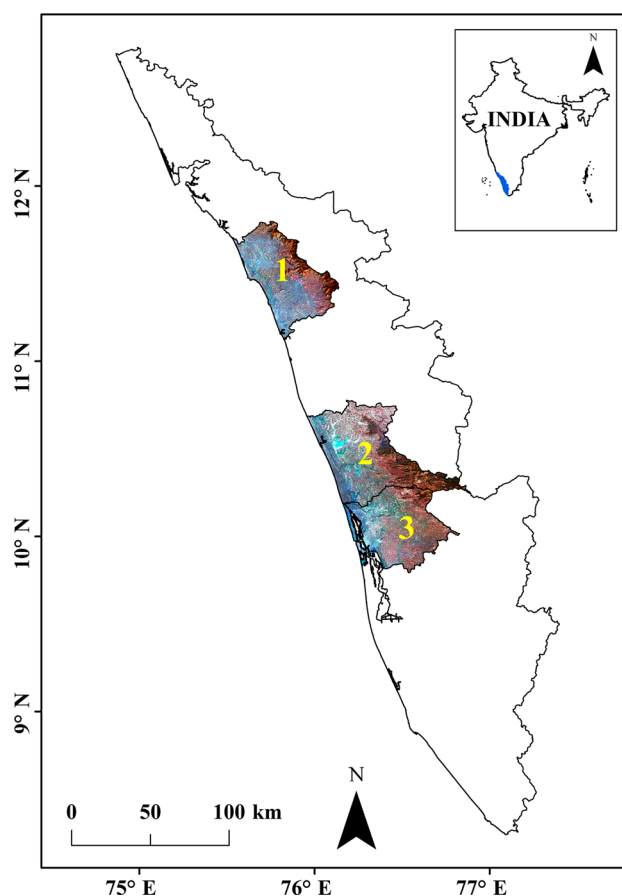


Fig. 1 Districts considered for study whose metropolitan regions were investigated (1 Kozhikode, 2 Trichur, 3 Ernakulam). Geographical location of Kerala state in India is shown in the inset (blue polygon)

120 m, 60 m and 100 m, respectively and are resampled to 30 m resolution. These images are available from the United States Geological Survey (<https://earthexplorer.usgs.gov/>) at no cost. All the images were taken from similar months (winter and/or autumn as urban heat islands (LST in this case) were observed to be stronger during this period). Details of Landsat data used for this study are summarized in Table 1.

Application of thermal imagery for estimating land surface temperature has been known since the 1970s (Chen et al. 2006). Since there is only one channel in the thermal region (for TM and ETM+), it is difficult to apply common temperature and emissivity retrieval methods using Landsat data (Liu and Zhang 2011). An alternative way is to calculate the emissivity of the surface from the normalized difference vegetation index (NDVI) and then use this NDVI to calculate surface temperature. The NDVI has been used very early as a major indicator of urban climate (e.g., Gallo et al. 1993) and indicators of UHI formation by urban researches (e.g., Yuan and Bauer 2007). The Landsat images were used to generate NDVI, which is later used to

Table 1 Details of Landsat data tested and used in this study

Sensor	Date of acquisition	Spatial resolution (m)	Path/row	Scene/product ID
OLI	02 February 2014	30, 100 (Thermal), 15 (PAN)	145/52	LC08_L1TP_145052_20140202_20170426_01_T1
OLI	27 December 2017	30, 100 (Thermal), 15 (PAN)	145/52	LC08_L1TP_145052_20171227_20180103_01_T1
OLI	25 October 2017	30, 100 (Thermal), 15 (PAN)	145/52	LC08_L1TP_145052_20171024_20171107_01_T1
OLI	18 January 2017	30, 100 (Thermal), 15 (PAN)	144/53	LC08_L1TP_144053_20170118_20170311_01_T1
OLI	13 January 2015	30, 100 (Thermal), 15 (PAN)	144/53	LC08_L1TP_144053_20150113_20170414_01_T1
ETM+	20 December 2000	30, 60 (Thermal), 15 (PAN)	145/52	LE07_L1TP_145052_20001220_20170208_01_T1
ETM+	26 October 2000	30, 60 (Thermal), 15 (PAN)	144/53	LE07_L1TP_144053_20001026_20170209_01_T1
ETM+	18 February 2002	30, 60 (Thermal), 15 (PAN)	144/53	LE07_L1TP_144053_20020218_20170201_01_T1
TM	10 March 1998	30, 120 (Thermal)	145/52	LT05_L1TP_145052_19980310_20161225_01_T1
TM	15 December 1995	30, 120 (Thermal)	145/52	LT05_L1TP_145052_19951215_20170105_01_T1
TM	03 February 1991	30, 120 (Thermal)	145/52	LT05_L1TP_145052_19910203_20170127_01_T1
TM	27 December 2008	30, 120 (Thermal)	144/53	LT05_L1TP_144053_20081227_20170111_01_T1
TM	11 March 2001	30, 120 (Thermal)	144/53	LT05_L1TP_144053_20010311_20161212_01_T1
TM	31 December 1992	30, 120 (Thermal)	144/53	LT05_L1TP_144053_19921231_20170120_01_T1

estimate emissivity (Sobrino et al. 2004) in the study area. Some images used to calculate LST were not used for estimating vegetation changes due to the presence of slight cloud cover in the image. Using emissivity and thermal infrared (TIR) bands of the satellite data, land surface temperatures of the area of interest were calculated. The entire process in detail with each step analyzed is shown in the flowchart given below (Fig. 2).

In the first step, digital number (DN) of the original images has been converted into the corresponding radiance using the conversion parameters corresponding to each sensor (i.e., TM, ETM+ or OLI). Atmospheric correction, which is used for attenuating the effects of atmospheric scattering caused by aerosols and suspended particles, for visible and shortwave infrared (SWIR) channels have been done separately from thermal channels. For thermal bands, major interference factor from the atmosphere is water vapor than suspended particles. Due to the lack of radiosonde data, application of more accurate methods of atmospheric correction such as FLASSH or MODTRAN was not possible. In this way, for the atmospheric correction in visible and the SWIR, QUAC (Atmospheric Correction—ENVI 5.3) method was used. This method performs the atmospheric corrections using the information extracted from the image itself, observing the spectral curve of each pixel for this, generating very accurate results for any solar elevation angle. For the atmospheric correction of the data in the TIR, the atmospheric parameters of upwelling radiation (Lu), downwelling radiation (Ld) and transmittance (t) were calculated with the Atmospheric Correction Parameter Calculator, which is a MODTRAN online module for LANDSAT (<https://atm.corr.gsfc.nasa.gov>). These parameters will be used later for

the atmospheric correction of the data simultaneously with the temperature calculation using a MATLAB script.

Once the atmospheric correction has been finished, subsets of the area of interests from multispectral and thermal images were created and the normalized difference vegetation indices have been extracted ($NDVI = [NIR - RED]/[NIR + RED]$) using ENVI 5.3. As given in Zhang et al. (2006) and later followed by Grondona et al. (2013), emissivity estimation using NDVI is given in Table 2. To perform the processing, a MATLAB algorithm was implemented, which processes the pixel-by-pixel data, determining the emissivity according to the NDVI value and Table 2.

In order to extract the LST, the radiance measured by the sensor in TIR (Chen and Cheng 2012) is given by Eq. 1:

$$L(\lambda, T) = [\varepsilon_{\lambda} B(\lambda, T) + (1 - \varepsilon_{\lambda}) Ld(\lambda)] \tau + Lu(\lambda) \quad (1)$$

where λ is the wavelength in μm , T is the temperature in Kelvin, $L(\lambda, T)$ is the thermal radiance for the temperature T in wavelength λ , ε_{λ} is the surface emissivity, $B(\lambda, T)$ is the Planck function for the blackbody for the temperature T in wavelength λ , $Ld(\lambda)$ is the downwelling radiation for wavelength λ , $Lu(\lambda)$ is the upwelling radiation for wavelength λ , τ is the atmospheric transmissivity for wavelength λ .

As the atmospheric parameters and emissivity have already been calculated, to determine the temperature it is enough to isolate the variable T that is on the right side of Eq. 1 as:

Fig. 2 Flowchart showing the steps for estimating UHI using Landsat data (*QUAC* Quick Atmospheric Correction, *NDVI* Normalized Difference Vegetation Index, *TIR* Thermal Infrared)

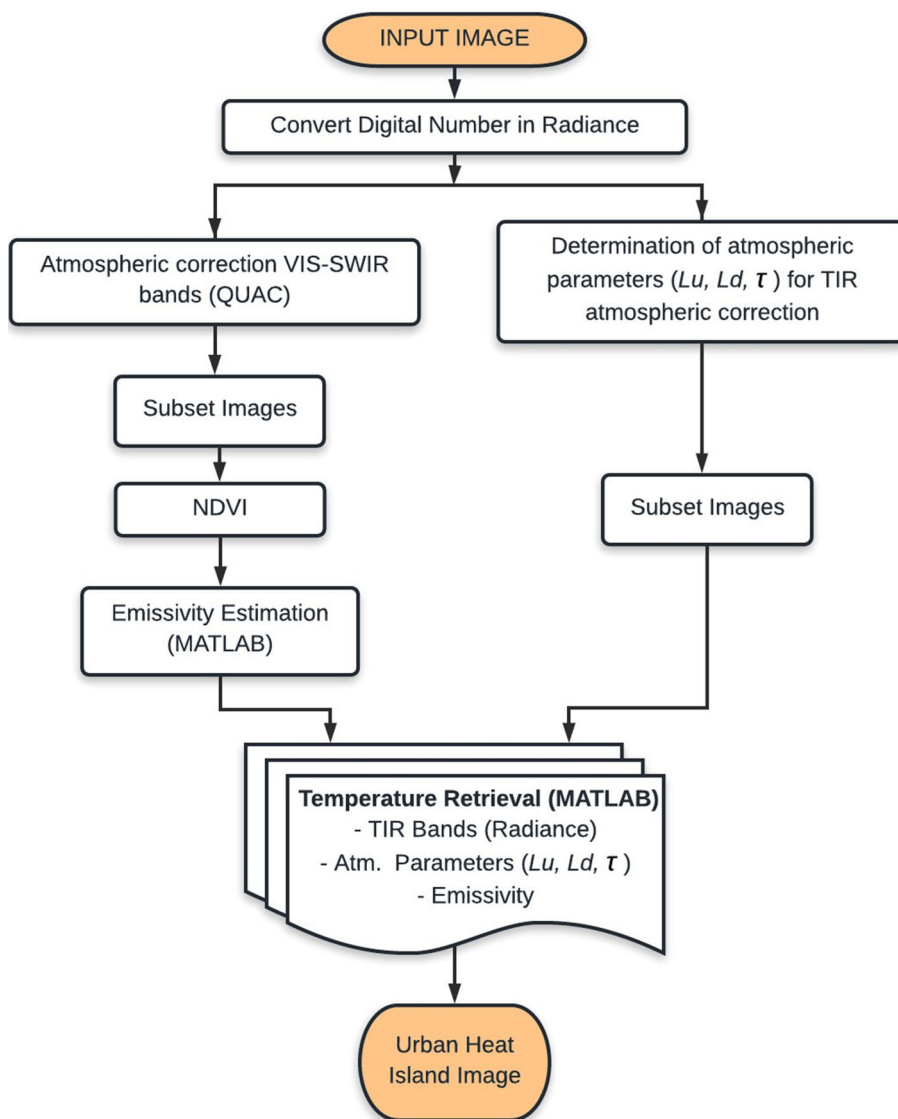


Table 2 Emissivity estimated from NDVI for Landsat data

NDVI	Land surface emissivity (ϵ_s)
$NDVI < -0.185$	0.995
$-0.185 \leq NDVI < 0.157$	0.970
$0.157 \leq NDVI \leq 0.727$	$1.0094 + 0.047 \ln(NDVI)$
$NDVI > 0.727$	0.990

$$T = \frac{C_1}{\lambda \ln \left(\frac{C_2}{\lambda^5 (L(\lambda, T) - Lu - \tau(1 - \epsilon_s)Ld) / \tau \epsilon_s} + 1 \right)} \quad (\text{W/m}^2 \text{ sr } \mu\text{m}) \tag{2}$$

Here, C_1 ($= 3.74151 \times 10^{-6} \text{ Wm}^2$) is the first radiation constant and C_2 ($= 0.0143879 \text{ mK}$) is the second radiation constant (Mohr et al. 2012; Yu et al. 2014).

One of the easiest and practical ways to map changes in vegetation from optical satellite data is using vegetation indices such as leaf area index (LAI) or NDVI (Fanfani et al. 2015; Gratani et al. 2015). Vegetation changes, which are mostly associated with anthropogenic activities such as urbanization or agricultural practices, during the study period, have been estimated using NDVI (Gandhi et al. 2015). NDVI images are easy to calculate and classify since the resultant normalized images are having significant differences in the DN values with different objects on the land surface. Change detection techniques discussed in Veettil (2012) were also applied to visually understand the growth of urbanization in the study site. Vegetated areas can be extracted from NDVI images by applying a suitable positive threshold value. Since the discrimination of vegetation types were not necessary, we used a minimum threshold value (> 0.2) to separate “vegetation” and “not vegetation” classes only.

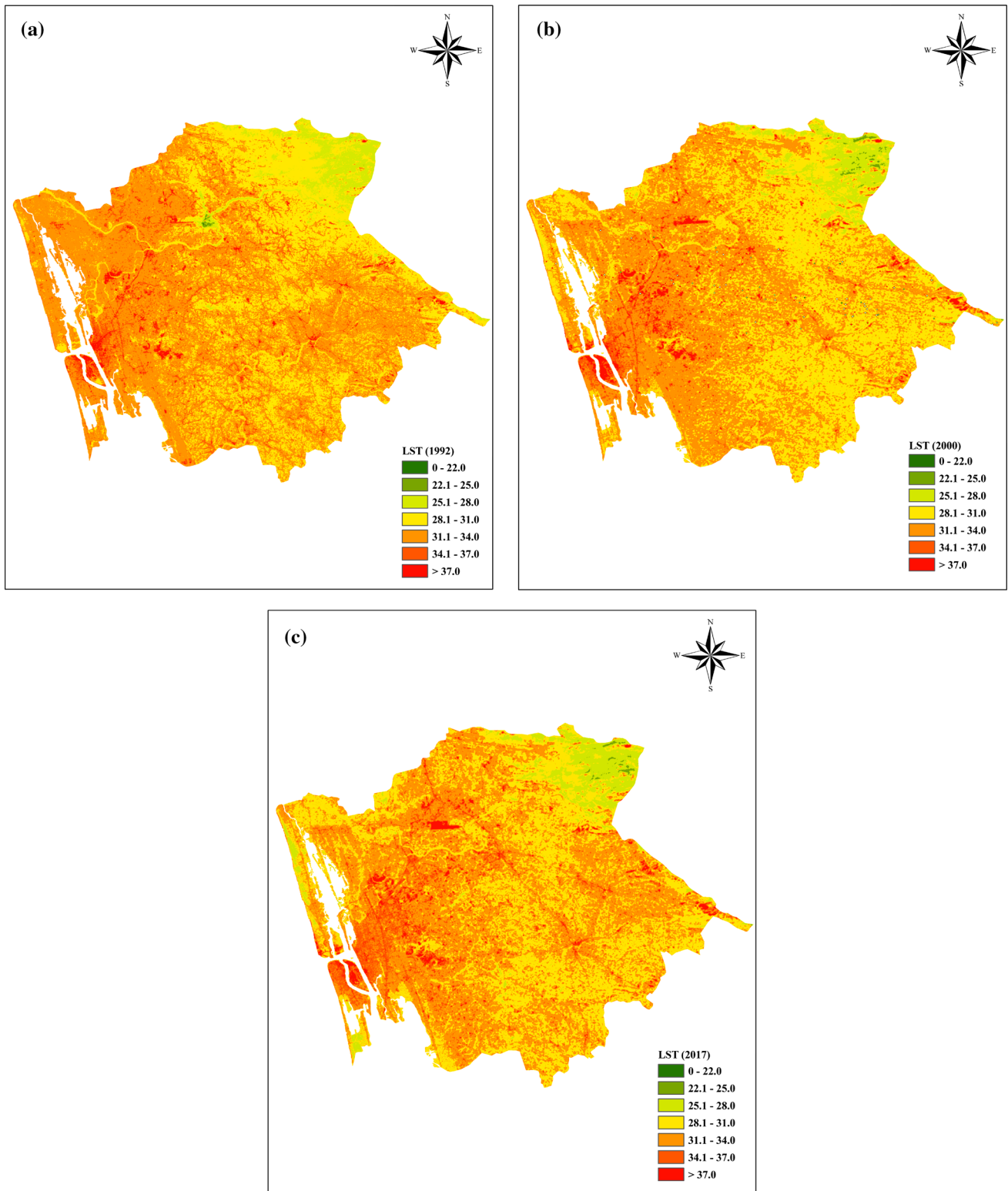


Fig. 3 LST in Ernakulam: a 1992, b 2000 and c 2017

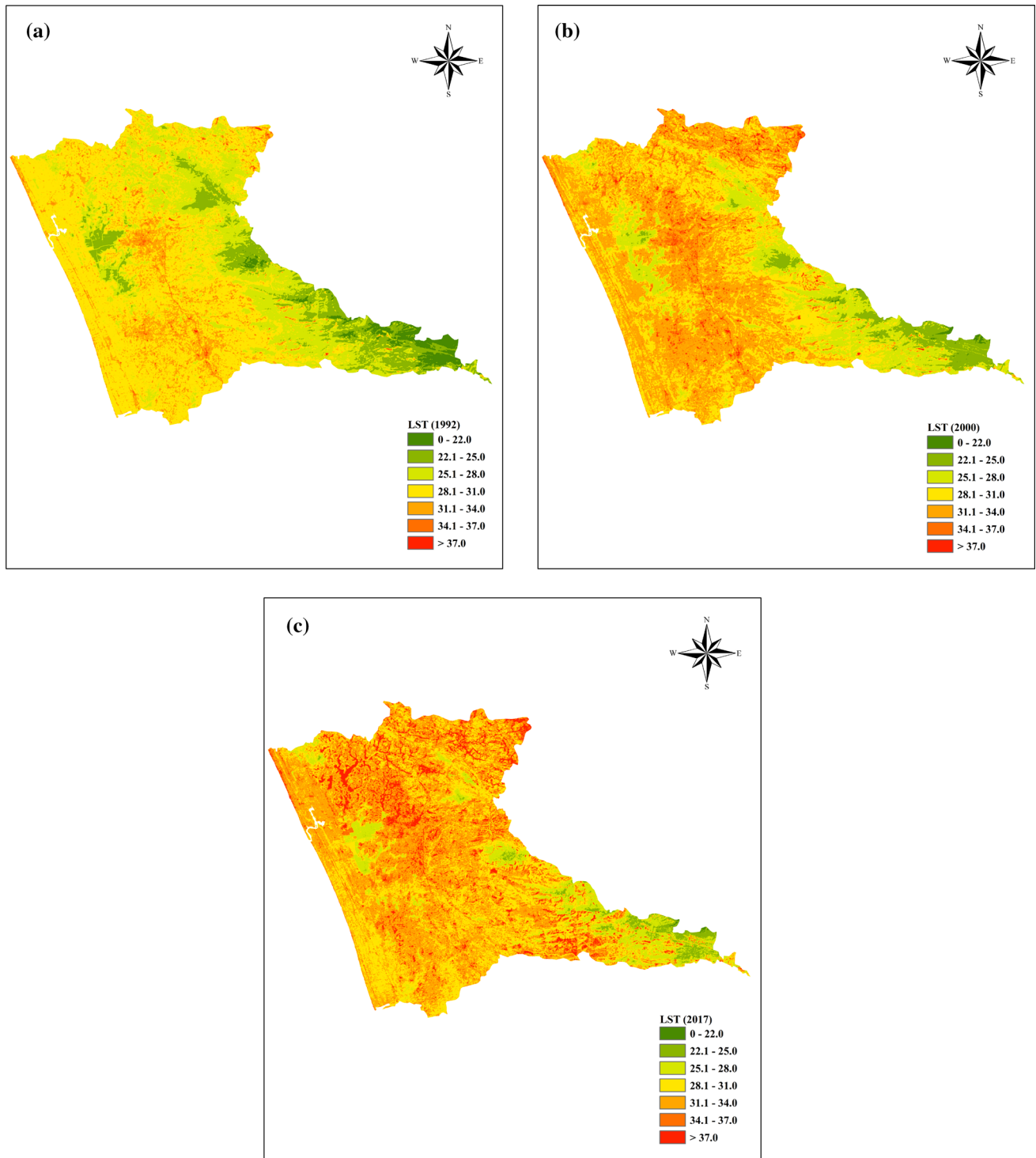


Fig. 4 LST in Trichur: a 1992, b 2000 and c 2017

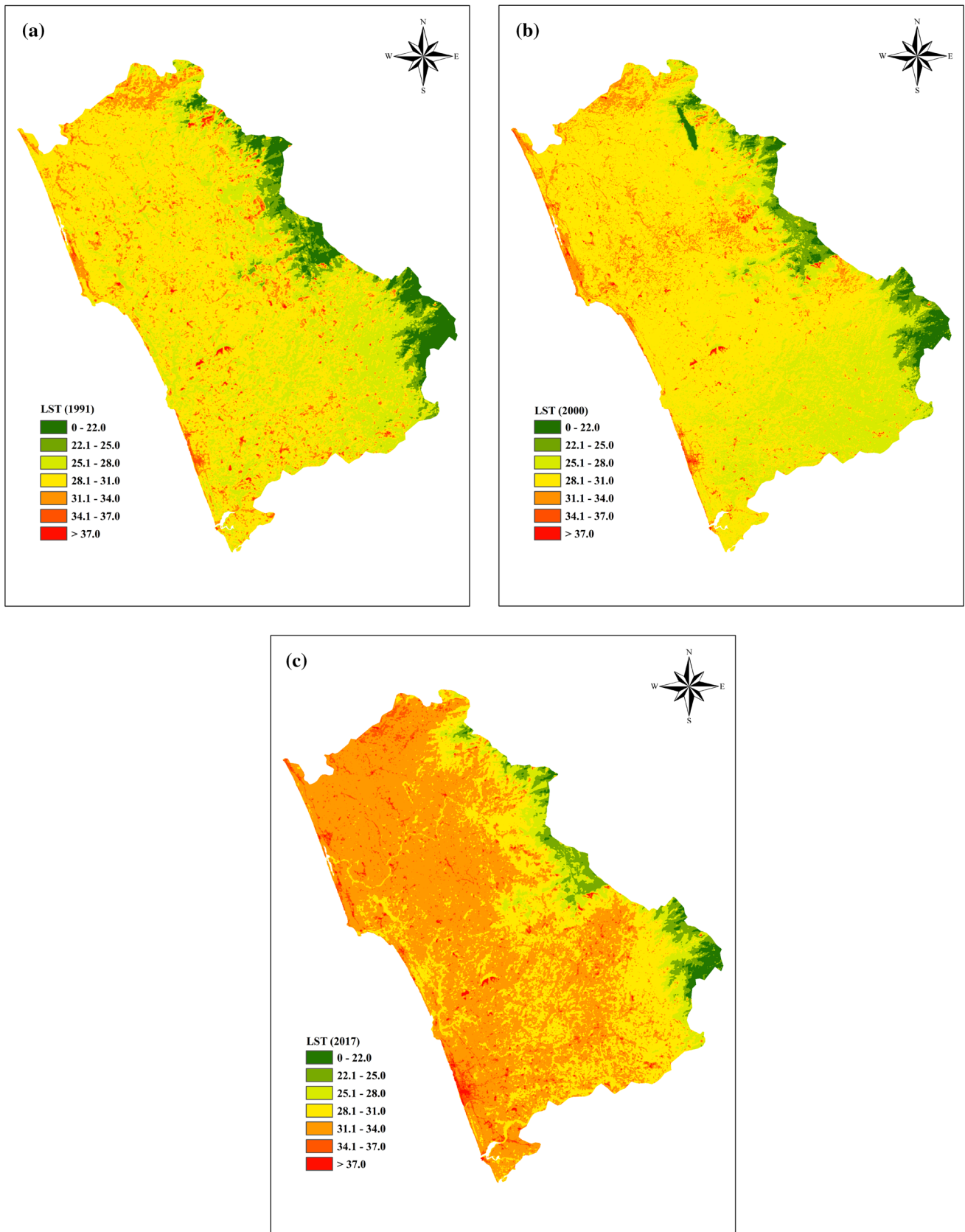


Fig. 5 LST in Kozhikode: a 1991, b 2000 and c 2017

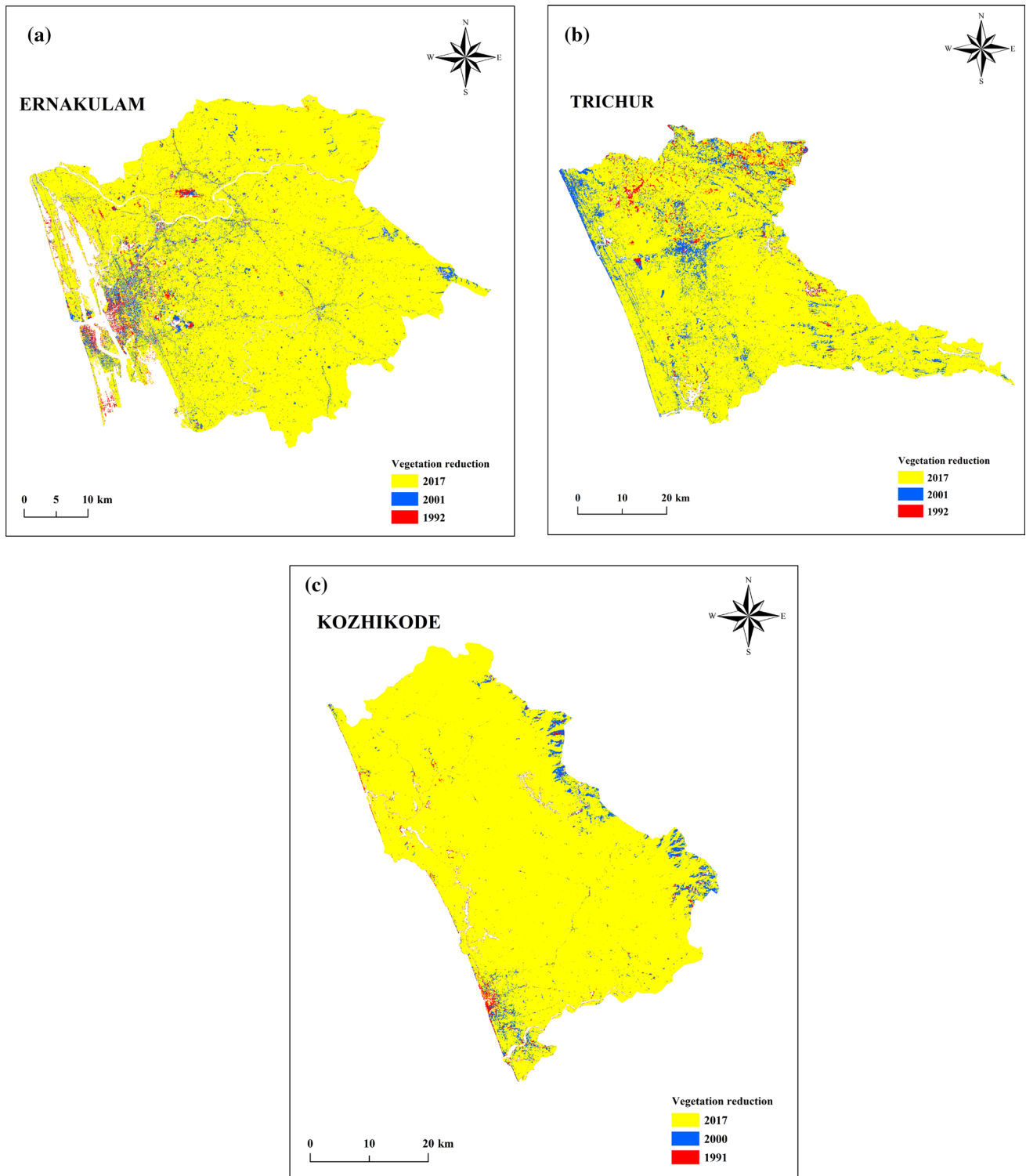


Fig. 6 Vegetation changes for the period 1991/1992–2017 in **a** Ernakulam, **b** Trichur, **c** Kozhikode

Results

Changes in land surface temperature (1991–2017)

Estimated changes in land surface temperatures showed that there was an overall increasing trend in the study areas between 1991 and 2017 (Figs. 3, 4, 5). However, these trends were not uniform. Highly urbanized regions in Ernakulam maintained a high LST with a gradual rise during the study period. However, rapidly urbanizing areas of Trichur and Kozhikode districts showed a higher increase in LST during the same period. It is also observed that human settlements and paved areas with asphalt and concrete showed a higher LST (more visible in Fig. 3) due to low surface albedo compared to vegetated surfaces that showed lower LSTs.

Changes in vegetation cover (1991–2017)

Estimated changes in vegetation showed a reduction in the vegetation coverage for Ernakulam, Trichur and Kozhikode districts as 5.8%, 10.38%, and 9.6%, respectively, for the period between 1991 and 2017 (Fig. 6). Observed vegetation coverage was: Ernakulam (1992: 2120.7 km², 2001: 2051.65 km², 2017: 1996 km²), Trichur (1992: 2714.2 km², 2001: 2537.2 km², 2017: 2432.2 km²), and Kozhikode (1991: 2134 km², 2000: 2051.4 km², 2017: 1927.35 km²). Higher loss of vegetation in Trichur and Kozhikode districts were due to rapid urban sprawl in the region compared to already urbanized areas in Ernakulam district.

As seen from the results, it is believed that the differences in the increase rate of LST is related to the changes in vegetation—higher loss of vegetation coverage was associated with higher changes in LST in Trichur and Kozhikode districts. The presence of vegetation reduces the surrounding temperatures through evapotranspiration and also due to shades by preventing solar radiation reaching the land surface (Senanayake et al. 2013a, 2013b). Figures 3, 4, 5 and 6 show that higher LST changes occurred near the areas where loss of vegetation occurs (i.e., build up areas). However, further investigations may be necessary to verify these changes using station data.

Last but not least, economic developments in Kerala, particularly in Kozhikode and nearby districts, are highly depending on immigrants to the Middle East (Zachariah and Rajan 2015). As the number of immigrants to the Middle East keep rising, economic growth since the 1980s keep rising (even though dependent on global recession) and have resulted in unprecedented increase in the number of urban settlements and utility vehicles, even though the state of Kerala is not considered as industrial friendly

(Zachariah and Rajan 2015). Other than urban growth rate, negative growth observed in paddy cultivation also indicates exploitation of agricultural lands for urban area expansion (Karunakaran 2014). These factors need to be taken into account while considering the urban growth and changes in LST in these regions.

Concluding remarks

This study was conducted to understand the vegetation changes and the evolution of land surface temperatures in three highly populated and rapidly urbanizing districts of Kerala state in south India using Landsat imagery. Results of this study derived the following conclusions:

- There was a gradual rise in the LST of Ernakulam district (vegetation loss 5.8%), where the region was already urbanized before the study period and still continuing the process of building new settlements in the suburban areas.
- In two districts (Trichur and Kozhikode), where occurring a rapid and continuing urbanization, vegetation loss during the study period was 10.4% and 9.6%, respectively.
- High rate of increase in the LST is believed to have associated with rapid urbanization process occurring in Kozhikode and Trichur districts whereas the gradual changes in LST observed in Ernakulam district might be due to the near saturation of or relatively slower urbanization process.
- Increase in population density and economic development in continuously urbanizing areas, particularly from the immigrants to the Middle East countries, is believed to be one of the reasons for urban growth in these regions.
- The methodology used in this study can be applied for any urban areas as it is easier to implement and the data used are available at no cost and hence affordable.

Acknowledgements Veetil BK acknowledges Ton Duc Thang University, Ho Chi Minh City, Vietnam, for research support. We are thankful to two anonymous reviewers for their valuable suggestions.

Compliance with ethical standards

Conflict of interest The authors declare that they have no conflict of interests.

References

- Carlson TN, Arthur ST (2000) The impact of land use—land cover changes due to urbanization on surface microclimate and

- hydrology: a satellite perspective. *Global Planet Change* 25:49–65. [https://doi.org/10.1016/S0921-8181\(00\)00021-7](https://doi.org/10.1016/S0921-8181(00)00021-7)
- Chen H-W, Cheng K-S (2012) A conceptual model of surface reflectance estimation for satellite remote sensing images using in situ reference data. *Remote Sens* 4:934–949. <https://doi.org/10.3390/rs4040934>
- Chen XL, Zhao HM, Li PX, Yin ZY (2006) Remote sensing image-based analysis of the relationship between urban heat island and land use/cover changes. *Remote Sens Environ* 104:133–146. <https://doi.org/10.1016/j.rse.2005.11.016>
- Cohen JE (2003) Human population: the next half century. *Science* 302:1172–1175. <https://doi.org/10.1126/science.1088665>
- Du P, Li X, Cao W, Luo Y, Zhang H (2010) Monitoring urban land cover and vegetation change by multi-temporal remote sensing information. *Min Sci Technol (China)* 20:922–932. [https://doi.org/10.1016/S1674-5264\(09\)60308-2](https://doi.org/10.1016/S1674-5264(09)60308-2)
- Estoque RC, Murayama Y (2014) Measuring sustainability based upon various perspectives: a case study of a hill station in Southeast Asia. *Ambio* 43:943–956. <https://doi.org/10.1007/s13280-014-0498-7>
- Fanfani A, Manes F, Moretti V, Ranazzi L, Salvati L (2015) Vegetation, precipitation and demographic response of a woodland predator: Tawny Owl *Strix aluco* as an indicator of soil aridity in Castelporziano forest. *Rend Lincei* 26:391–397. <https://doi.org/10.1007/s12210-015-0392-7>
- Gallo KP, McNab AL, Karl TR, Brown JF, Hood JJ, Tarpley JD (1993) The use of NOAA AVHRR data for assessment of the urban heat island effect. *J Appl Meteorol* 32:899–908. [https://doi.org/10.1175/1520-0450\(1993\)032<0899:TUONAD>2.0.CO;2](https://doi.org/10.1175/1520-0450(1993)032<0899:TUONAD>2.0.CO;2)
- Gandhi GM, Parthiban S, Thummalu N, Christy A (2015) NDVI: vegetation change detection using remote sensing and GIS—a case study of Vellore District. *Procedia Comput Sci* 57:1199–1210. <https://doi.org/10.1016/j.procs.2015.07.415>
- Gratani L, Bonito A, Crescente MF, Catoni R, Varone L, Tinelli A (2015) The use of maps as a monitoring tool of protected area management. *Rend Lincei* 26:325–335. <https://doi.org/10.1007/s12210-014-0355-4>
- Gronona AEB, Veettil BK, Rolim SBA (2013) Urban heat island development during the last two decades in Porto Alegre, Brazil, and its monitoring. In: *Proceedings of the joint urban remote sensing event (JURSE)*, Sao Paulo, Brazil, pp 61–64
- Karunakaran N (2014) Paddy cultivation in Kerala—trends, determinants and effects on food security. *Artha J Soc Sci* 13:21–36. <https://doi.org/10.12724/ajss.31.2>
- Liu L, Zhang Y (2011) Urban heat island analysis using the Landsat TM data and ASTER data: a case study in Hong Kong. *Remote Sensing* 3:1535–1552. <https://doi.org/10.3390/rs3071535>
- Mohr PJ, Taylor BN, Newell DB (2012) CODATA recommended values of the fundamental physical constants: 2010. *Rev Mod Phys* 84:1527–1605. <https://doi.org/10.1103/RevModPhys.84.1527>
- Ranagalage M, Estoque RC, Murayama Y (2014) An urban heat island study of the Colombo metropolitan area, Sri Lanka, based on Landsat data (1997–2017). *Int J Geo-Inf* 6(7):189. <https://doi.org/10.3390/ijgi6070189>
- Senanayake IP, Welivitiya WDDP, Nadeeka PM (2013a) Urban green spaces analysis for development planning in Colombo, Sri Lanka, utilizing THEOS satellite imagery—a remote sensing and GIS approach. *Urban For Urban Green* 12:307–314. <https://doi.org/10.1016/j.ufug.2013.03.011>
- Senanayake IP, Welivitiya WDDP, Nadeeka PM (2013b) Remote sensing based analysis of urban heat islands with vegetation cover in Colombo city, Sri Lanka using Landsat-7 ETM+ data. *Urban Clim* 5:19–35. <https://doi.org/10.1016/j.uclim.2013.07.004>
- Sobrino JA, Jiménez-Muñoz JC, Paolini P (2004) Land surface temperature retrieval from LANDSAT TM 5. *Remote Sens Environ* 90:434–440. <https://doi.org/10.1016/j.rse.2004.02.003>
- Son NT, Thanh BX (2018) Decadal assessment of urban sprawl and its effects on local temperature using Landsat data in Cantho city, Vietnam. *Sustain Cities Soc* 36:81–91. <https://doi.org/10.1016/j.scs.2017.10.010>
- Sudhira HS, Gururaja KV (2012) Population crunch in India: is it urban or still rural? *Curr Sci* 103:37–40
- UN (2016) The world's cities in 2016—data booklet (ST/ESA/SER.A/392). Department of Economic and Social Affairs, Population Division, United Nations, New York, p 29
- United Nations (UN) (2014) World urbanization prospects: the 2014 revision—highlights. United Nations, New York
- Veettil BK (2012) A comparative study of urban change detection techniques using high spatial resolution images. In: *Proceedings of the geographic object-based image analysis (GEOBIA)*, Rio de Janeiro, Brazil, pp 29–34
- Voogt JA, Oke TR (2003) Thermal remote sensing of urban climates. *Remote Sens Environ* 86:370–384. [https://doi.org/10.1016/S0034-4257\(03\)00079-8](https://doi.org/10.1016/S0034-4257(03)00079-8)
- Yu X, Guo X, Wu Z (2014) Land surface temperature retrieval from Landsat 8 TIRS—comparison between radiative transfer equation-based method, split window algorithm and single channel method. *Remote Sens* 6:9829–9852. <https://doi.org/10.3390/rs6109829>
- Yuan F, Bauer ME (2007) Comparison of impervious surface area and normalized difference vegetation index as indicators of surface urban heat island effects in Landsat imagery. *Remote Sens Environ* 106:375–386. <https://doi.org/10.1016/j.rse.2006.09.003>
- Zachariah KC, Rajan SI (2015) Dynamics of emigration and remittances in Kerala: results from the Kerala Migration Survey 2014. Working Paper No. 463, Centre for Development Studies, Thiruvananthapuram, Kerala, India
- Zhang Y, Yu T, Gu XF, Chen LF (2006) Land surface temperature retrieval from CBERS-02 IRMSS thermal infrared data and its applications in quantitative analysis of urban heat island effect. *J Remote Sens* 10:789–797